Kinetics of Cl Atom Reactions with C_2H_6, C_2H_5, and C_2H_4. Rates of Disproportionation and Recombination of Ethyl Radicals

Otto Dobis[†] and Sidney W. Benson*

Contribution from the Donald P. and Katherine B. Loker Hydrocarbon Research Institute, Department of Chemistry, University of Southern California, University Park, Los Angeles, California 90089-1661. *Received June 12, 1989*

Abstract: The kinetics of Cl atom reaction with ethane at 298 K were studied with the very low pressure reactor (VLPR). In the very early stages of reaction, with [Cl] > [C_2H_6], there is a very fast and irreversible reaction (1), producing HCl + C_2H_5 followed by a slightly slower reaction (2) of Cl with C_2H_5 to produce HCl + C_2H_4. An extremely slow reaction (4) of Cl with C_2H_4 to form HCl + C_2H_3 can also be seen followed by a much faster reaction (5) of Cl with C_2H_3 to form HCl + C_2H_2. After 50% Cl conversion when [Cl] < [C_2H_6], only reactions 1 and 3 (the disproportionation of C_2H_5) are important. By studying the reaction over large ranges of concentration of both Cl and C_2H_6, it is possible to obtain all rate constants except for (5) with good accuracy (cm^3/molecule·s × 10^{11}): $k_1 = 6.10 \pm 0.11$, $k_2 = 1.21 \pm 0.04$, $k_3 = 0.227 \pm 0.006$, $k_4 = 0.050 \pm 0.002$. Reaction 2 occurs via an initial recombination that is rate determining and can be described by the recently modified Gorin model for recombination. Ethyl radical disproportionation (3) is well described by a contact-transition-state model. From k_3 and the known ratio for disproportionation to recombination of 0.14 ± 0.01, the rate of recombination of ethyl radical at 298 K is calculated as $k_r = (1.62 \pm 0.14) \times 10^{-11}$ cm^3/molecule·s = $(9.7 \pm 0.8) \times 10^9$ L/mol·s.

The reactions of atomic chlorine with hydrocarbons have been extensively studied for various chemical and theoretical purposes for many years. Earlier investigations have been confined mainly to competitive chlorination techniques[1] and provided reliable kinetic data. In recent years, a renewed interest has been devoted to the systematic study of H atom metathesis by Cl atoms at low concentrations and at reduced pressures. These reactions are quenching processes in the stratographic ozone Cl chain reaction[2] initiated by anthropogenic chemicals. Although Cl reactions with H_2 and CH_4 are considered to be major sinks of Cl, since they are relatively abundant at stratospheric altitudes, other hydrocarbons and their halogen derivatives may also compete due to their much higher reactivity with Cl atom at stratospheric temperatures.

To obtain accurately measured rate constants for use in atmospheric models, improved techniques of kinetic measurements have been used. These include flash photolysis[3] combined with flow cell,[4] discharge flow tube,[5] all with time-resolved Cl resonance fluorescence analysis, as well as low-pressure rapid flow tube system with alternate mass spectrometry, and resonance fluorescence analysis.[6] All those kinetic methods have employed the pseudo-first-order approximation by measuring either the time-resolved relative fluorescence decay of Cl emission or the mass spectrometry signal of the substrate. Their results have been used as the "best" constants for Cl reaction of such substrates as H_2, CH_4, Cl_2O, ClO_2, etc.

The use of the pseudo-first-order approximation is only valid when the substrate concentration (RH) is essentially unchanged during the course of the reaction and no secondary reactions occur. This is generally not the case in the reactions of Cl atoms with C_2H_6 or higher hydrocarbons when very fast bimolecular Cl–radical processes as well as fast radical–radical reactions can occur. These can give rise to systematic errors and anomalies that have been reported. Such anomalies can be found in the slight pressure dependence of the rate constant of the Cl reaction with ethane in a flash photolysis system[3] and, to some lesser extent, as a flow rate dependence of the same rate constant when compared to the results obtained with flow cell[4] and discharge flow tube[5] kinetic techniques.

In principle, the interference of secondary reactions of products and intermediates can optionally be suppressed by reducing the initial concentration of the component undergoing first-order decay. In practice, it is a limited option, since its time-dependent concentration may quickly be reduced to the detection limit. Another remedy in fast-flow systems is to decrease the overall pressure of the system, but these increase the relative error of the rate constant measurement due to large corrections for radial diffusion and back-diffusion. It may also create slip flow. Increasing the flow rate can be accompanied by large pressure drops or, in the extreme, with violation of the conditions for Poiseuille flow.

All of these problems can be avoided by use of the VLPR (very low pressure reactor). By working in the millitorr pressure regime, we avoid complexities due to atom–radical and radical–radical recombination. By working with different orifices and, hence, different residence times, we can study extremely rapid reactions.

To face the problem of possible side processes outlined above, we have abandoned the pseudo-first-order approximation and varied the initial concentrations of both components over wide ranges. Simultaneous analysis of steady-state concentrations of both reactants and products was done by mass spectrometry with direct molecular beam sampling. This real second-order investigation creates some experimental difficulties in requiring the proper initial concentrations of reactants such that neither of them runs out of the well-measurable ranges.

In the Cl/C_2H_6 system, secondary reactions produce stable molecules C_2H_4 and C_2H_2 as well as HCl and measurable concentrations of C_2H_5 radicals. Mass spectrometric observations at all masses allow us to see all possible products of the reaction such as C_2H_5Cl, C_4H_{10}, $C_2H_4Cl_2$, etc. (none of which were observed), and to do mass balances on all species, thus making it possible to obtain an absolute mass spectrum of the ethyl radical.

Experimental Section

VLPR system is a versatile kinetic tool for the quantitative study of elementary fast reactions in the gas phase at low pressure. It is specially designed to eliminate a number of basic problems arising from viscous flow, diffusion, and other inhomogeneities of flow tube and non-steady-state reactors.[7] It falls into the category of flow cell reactor systems,

[†] Present address: Technical University of Budapest, H-1521 Budapest, Hungary.

(1) Fettis, G. C.; Knox, J. H. *Progr. Reaction Kinetics*; Porter, G., Ed.; Pergamon Press: New York, 1964; Vol. 2, p 1.
(2) Rowland, F. S.; Molina, M. J. *Rev. Geophys. Space Phys.* **1975**, *13*, 1.
(3) Davis, D. D.; Braun, W.; Bass, A. M. *Int. J. Chem. Kinet.* **1970**, *2*, 101.
(4) Manning, G.; Kurylo, M. J. *J. Phys. Chem.* **1977**, *81*, 291.
(5) Schlyer, D. J.; Wolf, A. P.; Gaspar, P. P. *J. Phys. Chem.* **1978**, *823*, 2633.
(6) Ray, G. W.; Keyser, L. F.; Watson, R. T. *J. Phys. Chem.* **1980**, *84*, 1674.

0002-7863/90/1512-1023$02.50/0

but having no flow velocity profile since it is a well-stirred reactor. This system has been successfully used for investigations of chlorine atom reactions and equilibria[8] earlier.

The system applied to the present study is a "three-chamber" variant; its technical parameters, use, and escape rate constant calculations are described in detail elsewhere.[9] The bottom of a Teflon-coated FEP-120 cylindrical reactor cell of 215.7-cm^3 volume is assembled on a quickly adjustable mechanism of three discharge orifices with diameters of 0.193, 0.277, and 0.485 mm. Further on, they are noted as ϕ_2, ϕ_3, and ϕ_5 in increasing order of sizes. The orifice changeover is executed from outside without breaking the vacuum, thus changing the steady-state concentrations in the reactor cell under fixed inlet conditions. With this reactor volume, the unimolecular escape rate constant is $k_{eM} = a_\phi(T/M)^{1/2}$ (s^{-1}), where T is the absolute temperature, M is the mass of any individual gas component present in the reactor cell, and $a_\phi = 0.285$ for ϕ_2, 0.546 for ϕ_3, and 1.321 for ϕ_5 orifices. The heating/cooling jacket of the reactor cell is connected to a constant-temperature bath circulator (Neslab RTE-5B), and the reactor temperature was kept at 25 ± 0.02 °C during all runs by monitoring the temperature with thermocouples at the inlet and outlet ports of the jacket.

A 4.5% Cl_2/He mixture was prepared in a storage bulb by prior direct measurement of the partial pressures of the components (both Matheson research-grade gases). It was flowed to the reactor cell through a flow subsystem, consisting of a 586-cm^3 buffer volume and 100-cm-length interchangeable capillary resistances of 0.203- and 0.356-mm internal diameter. Before being allowed enter in the reaction cell, the Cl_2 content underwent 100% dissociation in a McCarrol antenna cavity of Opthos microwave power generator operated at from 25 to 80 W of 2.45-GHz output. Complete dissociation of Cl_2 can be well controlled by the microwave power at up to 5 × 10^{15} molecules/s flow rate and is checked by mass spectrometry.

A 4.94% C_2H_6/He mixture was prepared in a similar way from Matheson research-grade ethane and fed in from a buffer volume of 604 cm^3 through 100-cm-length capillary resistance of 0.229-mm internal diameter. The upstream pressures of both feed lines were controlled by Validyne pressure transducers in a range between 10 and 40 Torr and kept constant during each run.

Results

Preliminary experiments on the Cl atom reaction with ethane disclosed that the primary step (1) of H atom metathesis is followed by two disproportionation steps. This suggests that at least the following three consecutive steps occur in the given system:

$$C_2H_6 + Cl \xrightarrow{k_1} HCl + C_2H_5 \quad (1)$$

$$C_2H_5 + Cl \xrightarrow{k_2} HCl + C_2H_4 \quad (2)$$

$$2C_2H_5 \xrightarrow{k_3} C_2H_6 + C_2H_4 \quad (3)$$

The considerable influence of reaction 3 can be well observed experimentally by increasing the residence time at constant inlet flow condition of the reactants. These tests indicated a clear-cut orifice dependency of Cl consumption on reaction 3. No traces of radical–radical or atom–radical combinations were ever found in our studies, e.g., n-C_4H_{10} or C_2H_5Cl.

Later on, the fourth step of

$$C_2H_4 + Cl \underset{}{\overset{k_4}{\rightleftharpoons}} HCl + C_2H_3 \quad (4)$$

was found necessary to fit the data at longer residence time. In spite of its slow rate, it can contribute especially at high conversion rates of ethane when ϕ_2 or ϕ_3 orifices were used to increase the residence time.

These secondary reactions make the interpretation of the mass spectra a complex task. Mass 30 can be uniquely assigned to C_2H_6, but both C_2H_5 and C_2H_6 contribute to mass 29 and also to mass 28 by fragmentation. To effect accurate assignments for each species, we made use of spectra measured at different energies of the ionizing electron beam.

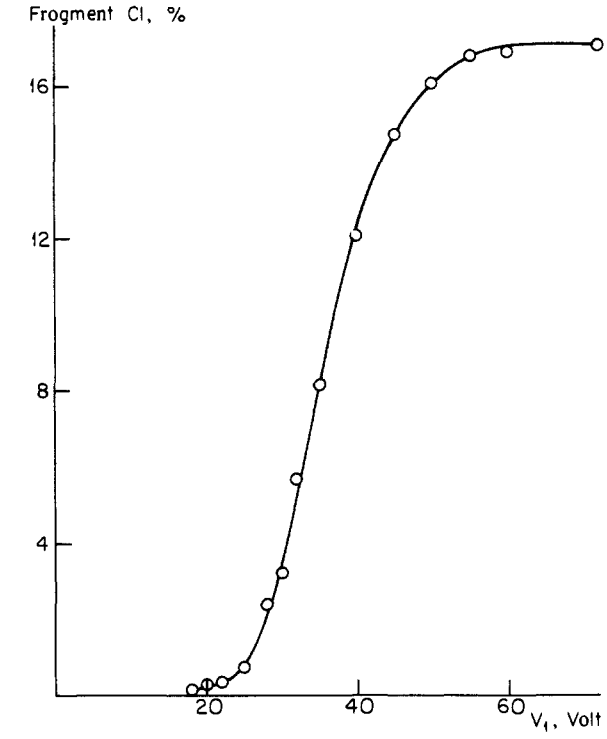

Figure 1. Percentage of HCl fragmentation (ordinate) as a function of the ionizing electron energy (abscissa) in the quadrupole mass analyzer recorded at 1.16 × 10^{13} cm^3/molecule·s specific flow rate of pure HCl.

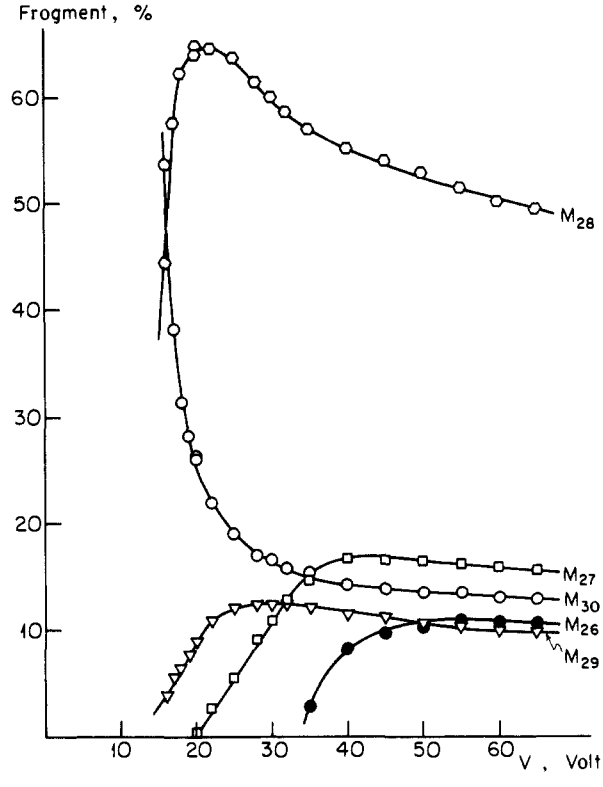

Figure 2. Mass spectra of ethane as a function of electron energy (abscissa) in the quadrupole mass analyzer at 1.46 × 10^{12} cm^3/molecule·s specific flow rate of 4.94% C_2H_6/He mixture. Ordinate: percentage of each peak.

Cl_2 is easily distinguished from Cl or HCl by the mass peaks at 70, 72, and 74. Similarly, HCl is easily measured by the parent peaks at masses 36 and 38. However, it contributes to the mass peaks at 35 and 37 used to measure Cl atoms. In Figure 1, we show the contribution of HCl fragmentation to mass 35 as a function of electron voltage. At 20 eV the fragmentation of HCl is 0.24%. Its absolute amount is usually much less than chlorine

(7) Golden, D. M.; Spokes, G. N.; Benson, S. W. *Angew. Chemie, Int. Ed. Engl.* **1973**, *12*, 534.
(8) Baghal-Vayjooee, M. H.; Colussi, A. J.; Benson, S. W. *Int. J. Chem. Kinet.* **1979**, *11*, 147. Heneghan, S. P.; Knoot, P. A.; Benson, S. W. *Int. J. Chem. Kinet.* **1981**, *13*, 677.
(9) Dobis, O.; Benson, S. W. *Int. J. Chem. Kinet.* **1987**, *19*, 691.

atoms consumed by reaction 4 in any of the experiments. For this reason, 20-eV electron energies were selected for recording Cl concentrations. Deviations in chlorine mass balance, $[Cl]_0 = [Cl] + [HCl]$, were found to be less than ±2% throughout the experiments.

Fragmentation of ethane is a more complex process as shown in Figure 2. At 20 eV, only two fragments at 28 and 30 account for 91% of the mass peaks. Mass 29 is only 9%, but the ethane decomposition is a steep function of the mean electron energy at 20 eV. However, if all voltages of the ion source are well optimized, so that the ion formation chamber works well within the oscillation stable area, the fragmentation ratios can be reproduced accurately with the reset of the ionization voltage. At 40 eV, the fragmentation of ethane is less sensitive to electron voltage and the signal is 3 times larger than at 20 eV, but two more fragments at 26 and 27 appear in the spectrum. To minimize the source of error due to fragmentation, mass scanning between m/e 26 and 30 was carried out at both ionization voltages, and the kinetic results obtained are presented with marked symbols in the figures.

Ethane flow rates versus mass spectral signal are presented in Figure 3a,b where the C_2H_6/He mixture prepared for experimentation was used. Each point is the average taken with all three discharge orifices. C_2H_6 spectra can be applied to the calculation of ethane concentrations directly.

By application of the steady-state condition to Cl, C_2H_6 (RH), and C_2H_5(Et), the following relations can be derived

$$2k_3[Et]^2 = k_1[RH][Cl] - (k_2[Cl] + k_{e\,Et})[Et] \quad (5)$$

$$[Et] = \frac{2\Delta[RH]k_{e\,RH} - k_1[RH][Cl]}{k_2[Cl] + k_{e\,Et}} \quad (5a)$$

$$[Et] = \frac{\Delta[Cl]k_{e\,Cl} - k_1[RH][Cl] - k_4[O1][Cl]}{k_2[Cl]} \quad (5b)$$

where $\Delta[RH] = [RH]_0 - [RH]$, the difference between the initial and final concentrations of ethane at any fixed flux setting for reactants. Note that the steady-state concentration of a reactant (RH) such as C_2H_6, in the absence of reaction, is given by $[RH]_0 = \Phi_{RH}/V_r k_{e\,RH}$ where Φ_{RH} is the flux and V_r is the reactor volume.

When (5a) and (5b) were equated, the kinetic equation for the difference in the relative consumption of chlorine and ethane takes the form

$$\frac{\Delta[Cl]}{[Cl]}k_{e\,Cl} - 2\frac{k_2[Cl]}{k_2[Cl] + k_{e\,Et}}\frac{\Delta[RH]}{[Cl]}k_{e\,RH} - k_4[O1] = k_1\left(1 - \frac{k_2[Cl]}{k_2[Cl] + k_{e\,Et}}\right)[RH] \quad (6)$$

Ethylene concentration [O1] can be derived from the steady-state conditions for C_2H_4 established by reactions 2–4 and by its escape rate that leads to the relationship

$$\Delta[Cl]k_{e\,Cl} - \Delta[RH]k_{e\,RH} = (2k_4[Cl] + k_{e\,O1})[O1] \quad (7)$$

k_4 is the smallest term in eq 7, of order 10^{-13}, so that $2k_4[Cl] \ll k_{e\,O1}$ and the ethylene concentration is given by

$$[O1] = \frac{\Delta[Cl]k_{e\,Cl} - \Delta[RH]k_{e\,RH}}{k_{e\,O1}} \quad (8)$$

Figure 4 shows that the approximation of eq 8 fits the data to better than 96% throughout the entire range of experiments. One consequence is that eq 7 cannot be used for the direct calculation of k_4 since it is not sensitive enough to k_4.

When eq 6 and 8 are combined, the explicit kinetic equation for the calculation of k_1 is

$$\frac{\Delta[Cl]}{[Cl]}k_{e\,Cl} - 2\frac{k_2[Cl]}{k_2[Cl] + k_{e\,Et}}\frac{\Delta[RH]}{[Cl]}k_{e\,RH} - k_4\frac{\Delta[Cl]k_{e\,Cl} - \Delta[RH]k_{e\,RH}}{k_{e\,O1}} = k_1\left(1 - \frac{k_2[Cl]}{k_2[Cl] + k_{e\,Et}}\right)[RH] \quad (9)$$

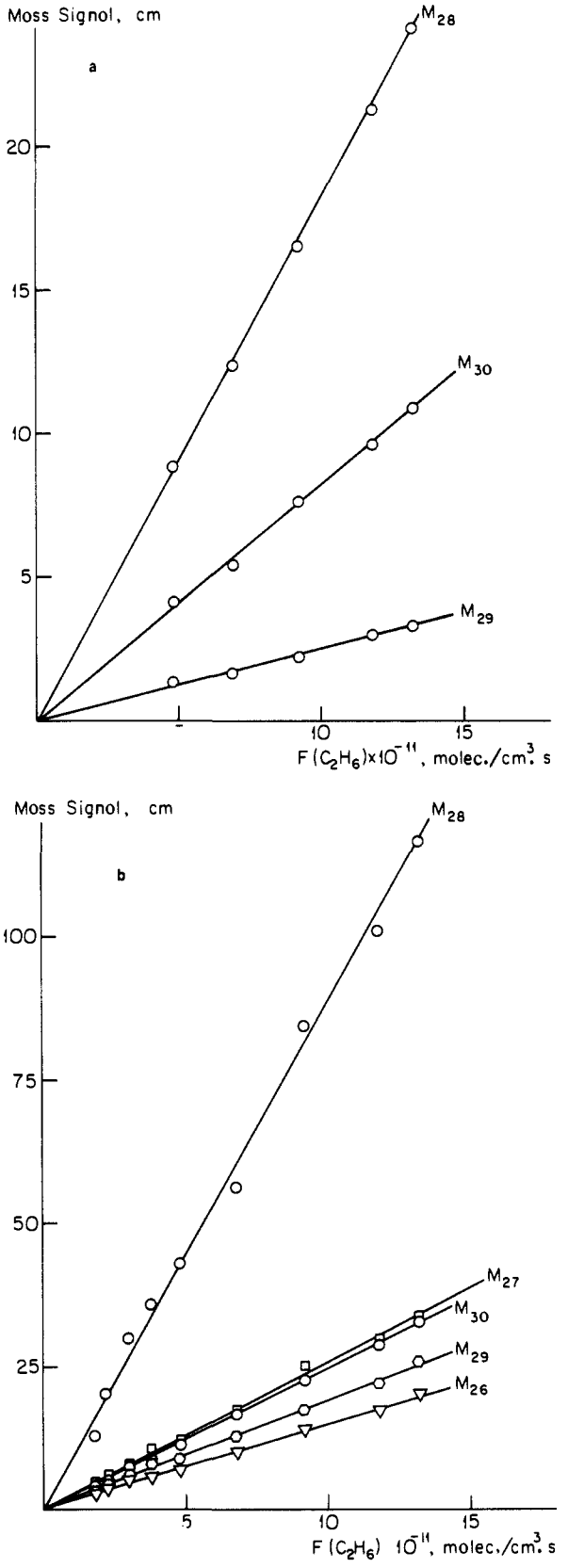

Figure 3. Mass spectra of ethane recorded at various specific flow rates (abscissa) of 4.94% C_2H_6 mixture: (a) at 20-eV ionization energy (1 cm = 0.15-eV signal display with beam modulation); (b) at 40-eV ionization energy.

Concentrations of the reactants are directly measurable quantities in each run, but the calculation of k_1 from eq 9 requires the knowledge of k_2 and k_4. Since there are no reliable direct relations for the calculation of these rate constants, their real values can optionally be approached by two separate linear regressions

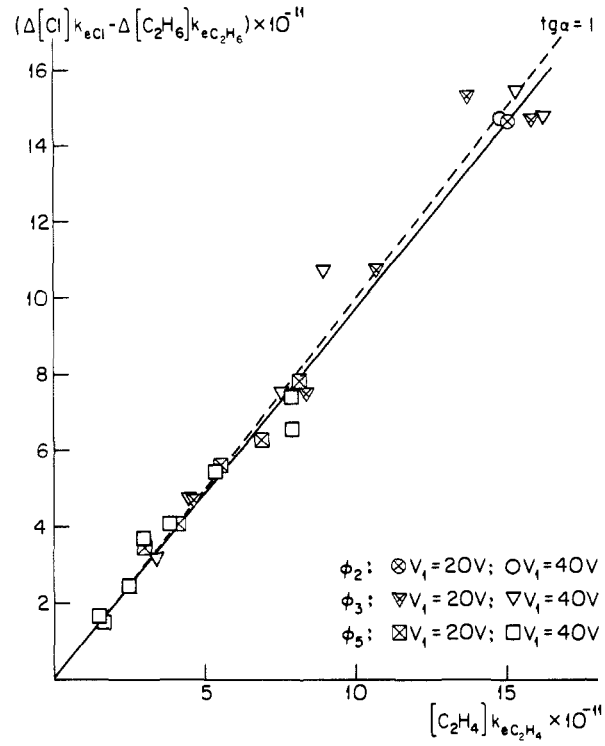

Figure 4. Mass balance between the consumption of reactants and ethylene formation approximated by eq 8. Dotted line shows the exact relationship by calculation. Orifices used for obtaining the given data pairs: ⊙, ϕ_2; ▽, ϕ_3; □, ϕ_5. Crossed symbols mark the results obtained with 20-eV mass ionization potential.

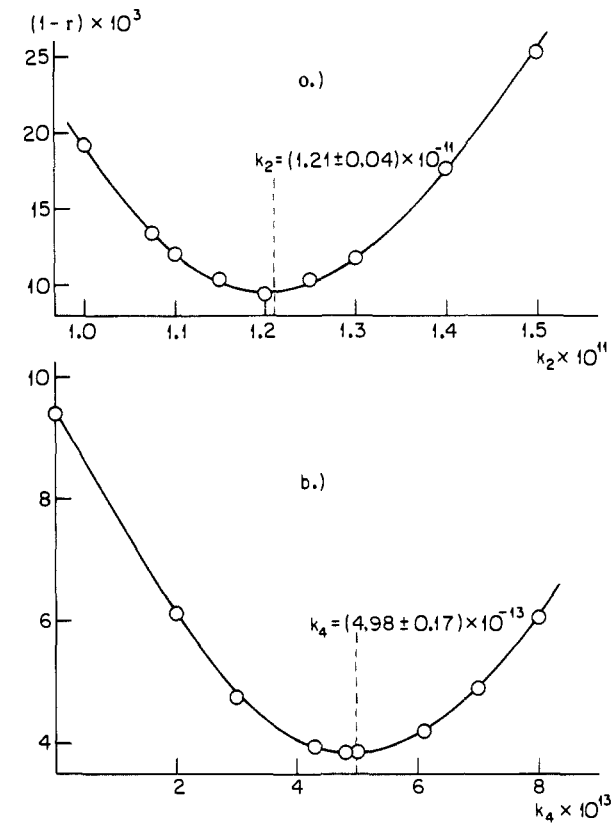

Figure 5. Sequences of regressions in calculations of k_2 (a) and k_4 (b). r is the coefficient of regression.

in the following way: the third term at the right side of eq 9 is small in comparison with the others, and it does not depend on k_2 directly. Therefore, it can be left off, and subjecting all concentration pairs experienced to linear regression around the expected value of k_2, the best fit of results is obtained with $k_2 = (1.21 \pm 0.04) \times 10^{-11}$ cm³/molecule·s. The sequel of this stepwise approach is illustrated in the upper part of Figure 5. Presentation of the kinetic results in Figure 6b, according to the incomplete form of eq 9, shows that the description of the system would relatively be poor without reaction step 4.

Repetition of regression according to the complete form of eq 9 with a now fixed value of k_2 gives $k_4 = (4.98 \pm 0.17) \times 10^{-13}$ cm³/molecule·s, as illustrated in the lower part of Figure 5.

With the above values of k_2 and k_4, the rate constant of chlorine atom reaction with ethane is found to be $k_1 = (6.10 \pm 0.11) \times 10^{-11}$ cm³/molecule·s, as shown in Figure 6a, over a relatively wide range of concentration variations. A simple comparison of Figure 6a with Figure 6b of the same scale exhibits the improvement in the reaction scheme by taking reaction step 4 into account. It is also worth noting that the chlorine atom driven disproportionation related to the discharge rate and expressed by $k_2[\mathrm{Cl}]/(k_2[\mathrm{Cl}] + k_{e\,\mathrm{Et}})$ was varied between 0.20 and 0.86 in the experiments.

The solution of eq 5 with the substitution of either eq 5a or 5b leads to identical functions for the calculation of k_3 in the knowledge of ethyl radical concentration. The first variant is the simplest one expressed in the form

$$\Delta[\mathrm{RH}]k_{e\,\mathrm{RH}} = k_3[\mathrm{Et}]^2 \qquad (10)$$

The mass spectrum of the ethyl radical registered during the reaction is not proportional to the radical concentration directly as it contains contributions from both the ethane and the ethyl radical fragmentation. There is no direct calibration to the relative flow rate or concentration of ethyl radicals. However, there is a good accordance of the ethane-related mass flow balance of pure fragmentation with combined reaction–fragmentation products, in spite of the quite different distribution of components in the two processes. These coincidences, presented in Figure 7a,b, suggest a reliable vertical unfolding of mass signals by taking advantage of the well-defined fragmentation functions given in Figure 3a,b. This signal unfolding proceeds as follows: first, the contributions of ethane fragmentation to each mass signal downward from $m/e = 29$ are calculated and subtracted, starting with the actual specific flow rate signal of C_2H_6 according to the C_2H_6 signal/flow relation of Figure 3a,b. If there were no reactions, the corresponding subtractions would have resulted in zero values of each signal from C_2H_5 down to C_2H_4 at 20-eV and to C_2H_2 at 40-eV electron energies. The residual signal of ethyl radical is reduced by its own fragmentation, which can be calculated by a second propagation downward, now starting with the M_{29} function of Figure 3a,b. In the case of 20-eV ionization (Figure 3a), this second reduction is just one step. The whole procedure can be followed graphically in the figures referred to. However, an analytical method was used for exact calculations.

To sum up the mass signal spectrum of ethyl radical obtained with the first and second subtractions, the specific flow rate of C_2H_5 in relation with ethane flow is established by the mass 29 relation of Figure 3a,b, which when divided by its escape rate constant, gives the radical concentration. In a similar way, summation of residual signals of $m/e = 26$–28 leads to the calculation of ethylene concentrations shown in the abscissa of Figure 4.

Ethyl radical concentrations obtained are plotted according to eq 10 in Figure 8, resulting in the ethyl radical disproportionation rate constant of $k_3 = (2.27 \pm 0.06) \times 10^{-12}$ cm³/molecule·s. The above method of unfolding can be applied with adequate accuracy when the residual radical signal obtained from the first subtraction constitutes at least 10% of the overall mass signal. Below that percentage, a second subtraction will result in a large scatter. While the experiments were designed to study the primary step of H metathesis, that falloff happened in only two runs with relatively high flow rates of ethane. These results are omitted from Figure 8.

Discussion

Kinetic investigation of Cl reaction with ethane is a more complicated task than with methane due to secondary disproportionation processes. Either of them is fast enough to compete

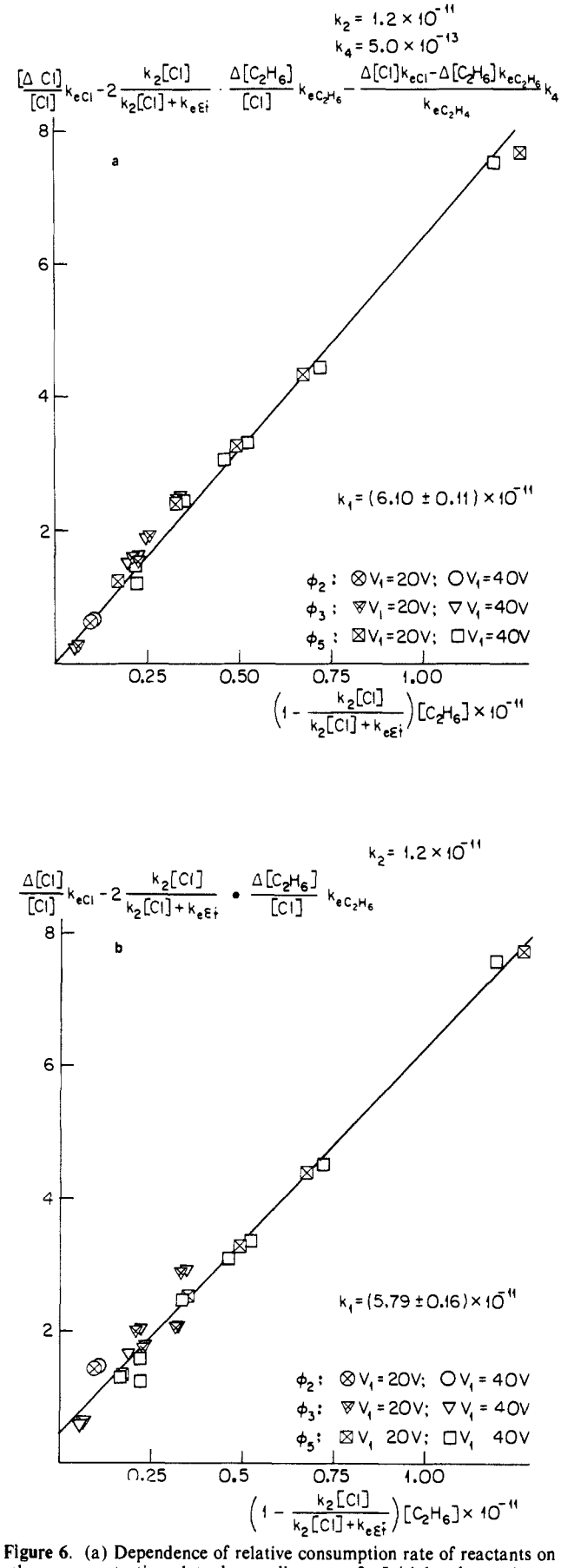

Figure 6. (a) Dependence of relative consumption rate of reactants on ethane concentration plotted according to eq 9. Initial and actual concentration ranges are $[Cl]_0 = (1.70\text{–}35.73) \times 10^{11}$, $[C_2H_6]_0 = (0.44\text{–}13.17) \times 10^{11}$, $[Cl] = (0.91\text{–}8.34) \times 10^{11}$, and $[C_2H_6] = (0.29\text{–}1.79) \times 10^{11}$ molecules/cm^3. Symbols of orifices are the same as in Figure 4. (b) Same as (a), but without reaction 4 of ethylene formed in the process.

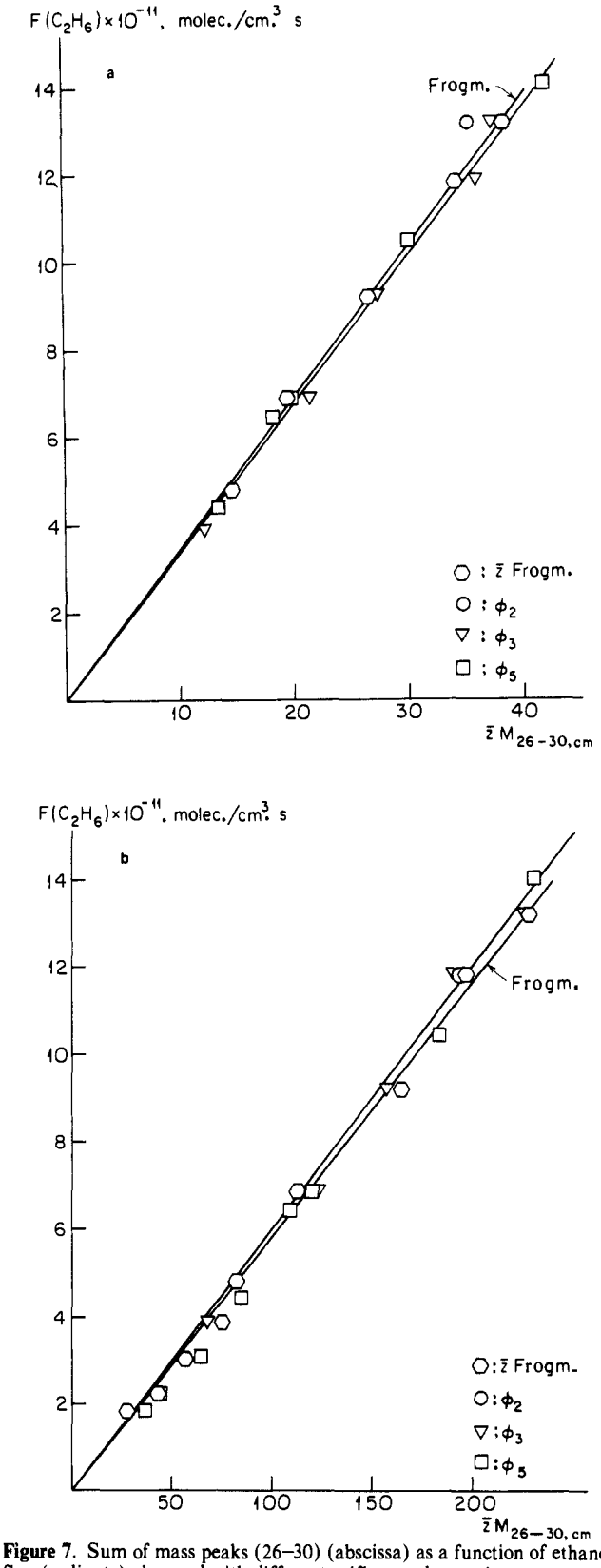

Figure 7. Sum of mass peaks (26–30) (abscissa) as a function of ethane flux (ordinate) observed with different orifices and at various extents of reaction with Cl. (a) Ionizing energy = 20 eV. ○ represents the sum of mass peaks, observed with no reaction. (b) Ionizing energy = 40 eV.

to some extent with the first-order-approximated decay of any of the two primary reactants used in excess in flow discharge systems. In low-pressure helium-diluted systems, they are the thermochemically probable channels for intermediates since the third-body requirement for recombination makes it very slow. The static system of flash photolysis[3] used in the overall pressure range 7–98 Torr found systematic variations in $k_1 = (6.5\text{–}7.3) \times 10^{-11}$ cm^3/molecule·s, a clear indication of a small interference by some

Table I. Comparison of Characteristics and Application Conditions of Flow Systems in Cl + C_2H_6 Studies

characteristic parameter	rapid discharge flow/mass spectrometry (ref 6)	rapid discharge flow/fluorescence emission (ref 5)	flow cell/fluorescence emission (ref 4)	VLPR (this work)
$\sum P_i$, Torr	1–2	3	5	(51–580) × 10^{-6}
F (conductance), cm³/s	(5.9–9.8) × 10^3	2.3 × 10^3	150	(0.36–168) × 10^3
Q (flow rate), cm³ Torr/s	(9.5–19.0) × 10^3	6.8 × 10^3	750	(1.8–97.5) × 10^{-2}
v (linear velocity), cm/s	1200–2000	2000	1.9	20.7–96.8
t (residence time), s	(2.5–40) × 10^{-3}	0.02	5.7	0.12–0.55
$\bar{\lambda}$ (mean free path), cm	(1.2–7.0) × 10^{-3}	4.7 × 10^{-3}	1.0 × 10^{-3}	16–180
ω (collision frequency), s^{-1}	(9–18) × 16^6	27 × 10^6	38 × 10^6	(5–55) × 10^2
$[Cl]_0/[C_2H_6]_0$	(2–3.5) × 10^{12}/ (7.5–38) × 10^{11}	(2–10) × 10^{11}/ (0.7–4.6) × 10^{12}	3 × 10^{-2}/10^{-5}	(1.7–36) × 10^{11}/ (6.4–13) × 10^{11}
carrier gas	He	He	Ar	He
k_1 × 10^{11} (at 298 K), cm/molecule·s	5.95 ± 0.28	4.0 ± 1.2	6.0 ± 0.8	6.10 ± 0.11

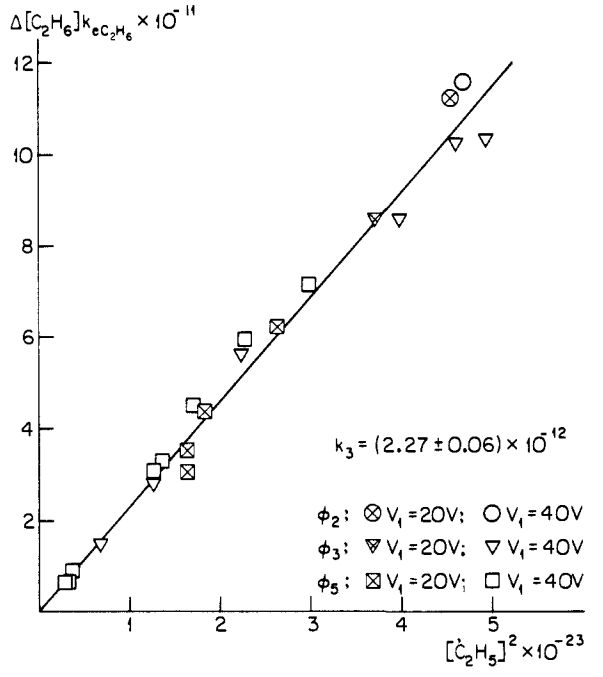

Figure 8. Square of ethyl radical concentration (abscissa) plotted according to eq 10, as a function of change in ethane flux (ordinate). Symbols of orifices are the same as in Figure 4.

side reaction in the Cl concentration decay. Therefore, it is not the correction of removing the self-absorption loss of Cl fluorescence intensity,[10] since that is a well-known and experimentally established fact,[11] but rather an extrapolation to low pressure that leads to the side reaction free area. From the extrapolation with the data of 7–15 Torr, k_1 = 6.15 × 10^{-11} cm³/molecule·s is obtained in excellent agreement with our result.

Table I summarizes the main gas dynamic characteristics of some flow systems used in investigations of the Cl reaction with ethane. The overall collision number is about 10^3 times less in the VLPR system than in the other systems. This enabled us to follow the side processes of intermediates and of ethylene product, thereby separating the perturbations of all side processes even those with rate constants 100 times less than that of the primary H-abstraction process. Our k_1 values are in excellent agreement with those reported in ref 3, 4, and 6. The initial concentration ratios of components set in the experiments of ref 5 are apparently not adequate for pseudo-first-order approximation of Cl decay. Furthermore, a flow tube of somewhat larger diameter should have been used to double, at least, the overall flow conductance of the system.

The usual tight transition state with a nonlinear Cl···H···C structure is shown in Figure 9. The deviation from a linear

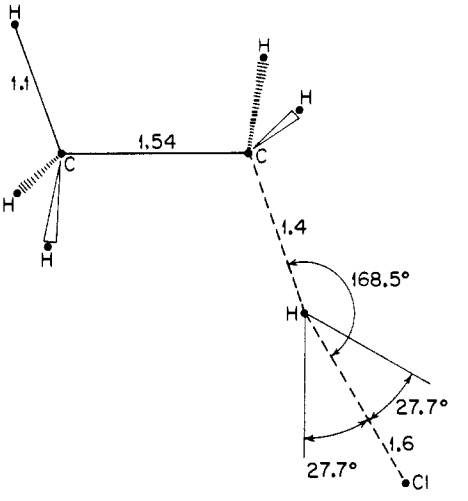

Figure 9. Configuration of the C_2H_6 + Cl transition-state model.

structure can extend to 27° before the Cl atom makes van der Waals contact with an adjacent atom. Using the methods developed for such a calculation,[12] one calculates an Arrhenius A factor of A_1 = 5.9 × 10^{-11} cm³/molecule·s with an uncertainty of about a factor of 2. This is sufficiently close to the measured value of the rate constant k_1 = 6.1 × 10^{-11} to suggest an activation energy very close to 0 ± 0.4 kcal. Both A factor and activation energy are in excellent agreement with recent measurements.[13]

There are no direct experimental measurements on the disproportionation or recombination of Cl atoms with ethyl radicals, not even for their ratio. The disproportionation is a relatively fast process that originates in the process of atom–radical recombination:

$$Cl + C_2H_5 \underset{-a}{\overset{a}{\rightleftharpoons}} (C_2H_5Cl)^* \xrightarrow{b} HCl + C_2H_4 + 66.7 \text{ kcal/mol}$$

Under VLPR conditions it can be shown that step b in this sequence is much faster than step −a ($k_b \gg k_a$) so that step a, the room-temperature recombination, becomes the rate-determining step. It is of interest to note that the pyrolysis of C_2H_5Cl that has been measured experimentally in the range 400–1130 °C has never been observed to produce radicals in competition with the much lower activation channel forming HCl + C_2H_4.[14] The enthalpy change in step a is −84.8 kcal/mol at 298 K while the energy change is 83.2 kcal/mol. All of this energy would have to be localized in the C–Cl bond in order for step −a to occur. In contrast only 56 kcal/mol, the activation energy for step b, need

(10) Watson, R. T. *J. Phys. Chem. Ref. Data* **1980**, *9*, 295.
(11) Braun, W.; Carrington, T. *J. Quant. Spectrosc. Radiat. Transfer* **1969**, *9*, 1113.
(12) Benson, S. W. *Thermochemical Kinetics*, 2nd ed.; Wiley: New York, 1976.
(13) Baul, B. L.; Cox, R. A.; Hampson, R. F.; Kerr, J. A.; Troe, J.; Watson, R. T. *J. Phys. Chem. Ref. Data* **1984**, *13*, 1259.
(14) Benson, S. W.; O'Neal, H. E. *Kinetic Data on Gas Phase Unimolecular Reactions*; National Standard Reference Data Service (U. S. National Bureau of Standards 21: Washington, DC, 1970; p 65. Heydtmann, H.; Dill, B.; Fonas, R. *Int. J. Chem. Kinet.* **1975**, *7*, 973.

be localized in the appropriate bonds for step b to occur. Although step −a has an estimated A factor of about $10^{15.2}$ s^{-1} while step b has an observed A factor of about $10^{13.6}$ s^{-1} extra entropy in the transition state of step b arising from R ln W, where W is the number of ways of distributing the excess internal energy, 83.2–56 = 27 kcal/mol, overwhelmingly favors step b over step −a.

An estimate of the rate of step a or step 2 is most easily made from the modified Gorin model for a loose transition state.[15] The rate is given by

$$k_2 = g_e\pi(b^*)^2\bar{v}_r\alpha \qquad (11)$$

where g_e is the ratio of electronic partition functions $g_e(EtCl)^*/g_e(Cl)g_e(Et)$, b^* is the Boltzmann-averaged impact parameter for the collision,[15] $\bar{v}_r$ is the relative velocity of the colliding pair, and α is the product of fractional "free areas" contributed by each of the reactants as their own active surface fractions occupied by free electron densities.

From the connected result of ref 15 (eq 11)

$$b^*/r_0 = 1.44(V_0/RT)^{1/4} \qquad (12)$$

where V_0 is the potential energy for the dissociation at 0 K. Correcting the dissociation energy of C–Cl bond to 0 K and adding zero-point energy differences, $V_0 \simeq 85$ kcal/mol. At 298 K, eq 12 then gives $b^*/r_0 = 3.29$ with $r_0 = 1.78$ Å and $b^* = 5.85$ Å. With $\bar{v}_r = 4.46 \times 10^4$ cm/s at $T = 298$ K and $g_e = 1/8$, eq 11 gives $\alpha = 0.2$ for the product of active surface fractions. By definition, $\alpha = \beta_{Et}\beta_{Cl}\beta_{Et} = 0.42$ is deduced from the data on recombination of ethyl radicals,[15] and with $\beta_{Cl} = 1$, since orientation effects of the Cl atom are included in g_e, we find $k_2 = 2.5 \times 10^{-11}$ cm^3/molecule·s, about a factor of 2 higher than the experimental result.

From the experimental value of k_2, or actually k_a for the recombination, one can also calculate k_{-a} the rate constant for the reverse process, the fission of C_2H_5Cl. At room temperature the entropy change in the fission is given by $\Delta S^\circ_{-a} = 32.0$ eu. Since by detailed balancing

$$K_a = \frac{k_a}{k_{-a}} = e^{\Delta S^\circ_a/R}e^{-\Delta H^\circ_a/RT} \qquad (13)$$

we see that

$$k_{-a} = k_a e^{-\Delta S^\circ_a/R}e^{\Delta H^\circ_a/RT} \qquad (14)$$

If we use the simple Arrhenius form for $k_{-a} = A_{-a}e^{-E_{-a}/RT}$ and neglect any small temperature dependence of k_a at 298 K, then $E_{-a} = -\Delta H_a$ and $A_{-a} = k_a e^{-E_{-a}/RT}$. When corrections are made to molecules per cubic centimeter standard state, we find that $A_{-a} = 1.1 \times 10^{15}$ s^{-1} and E_{-a} is just the energy change in the fission process. It is difficult to visualize an experimental method to measure k_{-a} so that this calculated value may never suffer from comparison with experimental observation.

With the exception of some high-temperature pyrolysis studies,[16] there are no direct experimental data for ethyl radical disproportionation; however, the disproportionation–combination ratio is well studied over a broad temperature range[17] in both the gas phase and solvent. A mean of recent data, in the range 290–410 K obtained with different kinetic methods and reported by different authors, gives $k_d/k_c = 0.14 \pm 0.01$.

By following the decay of ethyl radicals in the VLPR system with mass spectrometry measurement, we were able to obtain their disproportionation rate constant without any interference of other radical–radical decay processes, such as recombination. This rate constant is considerably less than k_2, but this reaction proceeds with direct H abstraction from one of the methyl groups through a "contact" transition-state mechanism. Reference 15 gives a detailed theoretical model of this reaction, yielding $k_d = 2.35 \times 10^{-12}$ cm^3/molecule·s, in excellent agreement with the present experimental value.

The above k_d/k_c ratio can now be used for checking the rate constant of ethyl radical recombination, current values for which vary by 2 orders of magnitude[17] (from 4.2×10^{-13} to 1.3×10^{-11} cm^3/molecule·s). The recalculation gives $k_c = 1.62 \times 10^{-11}$ cm^3/molecule·s, about half the value of the recombination rate constant for methyl radicals. This value is in comparatively good accord with $k_c = 1.4 \times 10^{-11}$ cm^3/molecule·s reported from molecular-modulation spectrometry studies of ethyl radical absorption at 280-nm wavelength[18] at room temperature. However, if the rate constant of disproportionation reported here is used to correct the sum $(k_c + k_d)$ given in ref 18, we find $k_c = 1.7 \times 10^{-11}$ cm^3/molecule·s, an improved agreement.

Our rate constant $k_4 = 5.00 \pm 0.17 \times 10^{-13}$ cm^3/molecule·s is in excellent agreement with the value of 4.87×10^{-13} cm^3/molecule·s obtained in a direct study of the Cl + C_2H_4 reaction at 298 K in VLPR.[19]

Conclusions

The present study demonstrates that the VLPR system can be used for the direct investigation of fast bimolecular reactions by varying the initial concentrations of both reactants. No approximations are necessary if concentrations are measured. Fast consecutive side reactions, like atom–radical and radical–radical disproportionations, cannot be eliminated by reducing the pressure or the residence time, but they can be well separated and their rate constants measured with adequate accuracy. Thus, the system provides kinetic measurement for interesting processes that can hardly be investigated otherwise. To do so, the residence time variation with outlet orifice changeover technique and the low-pressure characteristics of the system proved to be of practical benefit.

The analysis of boundary concentration conditions of the entire reaction system reveals that when Cl is used in excess (the case of resonance fluorescence/discharge technique), reactions 1 and 4 are measurable. Since k_1 and k_4 differ by 2 orders of magnitude, the kinetics of the two processes can be well separated by proper regulation of the residence time. The use of a large excess of Cl, which is required for the pseudo-first-order approximation, will hinder the determination of k_1 as the factor multiplying the ethane concentration in eq 9, $1 - k_2[Cl]/(k_2[Cl] + k_{e\,Et})$, tends to zero. On the other hand, when C_2H_6 is used in excess (mass spectrometry/discharge technique), reactions 1, 3, and 4 will become the major processes, where reaction 3 is much less separable from reaction 1 than reaction 4 by residence time regulation. Moreover, the determination of k_1 will depend on the term of $k_3k_4[C_2H_5]^2$, which is usually not a negligible fraction of $k_1[Cl]_0$.

Acknowledgment. This work has been supported by a grant from the National Science Foundation (CHE-87-14647).

Registry No. Cl, 22537-15-1; C_2H_6, 74-84-0; C_2H_5•, 2025-56-1; C_2H_4, 74-85-1; C_2H_3•, 2669-89-8.

(15) Benson, S. W. *Can. J. Chem.* **1983**, *61*, 881.
(16) Pacey, P. D.; Wilmalasena, J. H. *J. Phys. Chem.* **1984**, *88*, 5657. Kolke, T.; Gardiner, W. C. *J. Phys. Chem.* **1980**, *84*, 2005.
(17) *CRC Handbook of Biomolecular and Termolecular Gas Reactions*; Kerr, J. A., Ed.; CRC Press, Inc.: Boco Raton, FF, 1981; Vol. 2, p 80.
(18) Parkes, D. A.; Quinn, C. P. *J. Chem. Soc., Faraday Trans. 1* **1976**, *72*, 1952.
(19) Parmar, S. S.; Benson, S. W. *J. Phys. Chem.* **1988**, *92*, 2652.